A 424-year tree-ring based PDSI reconstruction of *Cedrus deodara* D. Don from Chitral

HinduKush Range of Pakistan: linkages to the ocean oscillations

Sarir Ahmad[1, 2], Liangjun Zhu[1, 2], Sumaira Yasmeen[1, 2], Yuandong Zhang[3], Zongshan Li[4], Sami

Ullah[5], Shijie Han[6, *], Xiaochun Wang[1, 2,*]

[1] Center for Ecological Research, Northeast Forestry University, Harbin 150040, China

[2] Key Laboratory of Sustainable Forest Ecosystem Management-Ministry of Education, School

of Forestry, Northeast Forestry University, Harbin 150040, China

[3] Key Laboratory of Forest Ecology and Environment, State Forestry Administration, Institute of

Forest Ecology, Environment and Protection, Chinese Academy of Forestry, Beijing 100091,

China

[4] State Key Laboratory of Urban and Regional Ecology, Research Center for Eco-Environmental

Sciences, Chinese Academy of Sciences, Beijing 100085, China

[5] Department of Forestry, Shaheed Benazir Bhutto University, Sheringal, Dir Upper, Pakistan

[6] State Key Laboratory of Cotton Biology, School of Life Sciences, Henan University, Kaifeng

475001, China

Corresponding authors: Xiaochun Wang, E-mail: wangx@nefu.edu.cn and Shijie Han, E-mail:

hansj@iae.ac.cn

Abstract. Currently, the rate of global warming has led to persistent drought patterns. It is

considered to be the preliminary reason affecting socio-economic development under the

background of dynamic forecasting of water supply and forest ecosystems in West Asia.

24 However, long-term climate records in the semi-arid Chitral Mountains of northern Pakistan are

25 seriously lacking. Therefore, we developed a new tree-ring width chronology of *Cedrus deodara*

26 spanning the period of 1537-2017. We reconstructed the March-August Palmer Drought

27 Sensitivity Index (PDSI) for the past 424 years back to A.D. 1593. Our reconstruction was

28 featured with nine dry and eight wet periods 1593-1598, 1602-1608, 1631-1645, 1647-1660,

29 1756-1765, 1785-1800, 1870-1878, 1917-1923, 1981-1995, and 1663-1675, 1687-1708, 1771-

30 1773, 1806-1814, 1844-1852, 1932-1935, 1965-1969 and 1996-2003, respectively. This

31 reconstruction is consistent with other dendroclimatic reconstructions in west Asia, confirming

32 its reliability. The analysis of multi-taper method and wavelet analysis revealed drought

33 variability at periodicities of 2.1-2.4, 3.3, 6, 16.8, and 34-38 years. The drought patterns could be

34 linked to the broad-scale atmospheric-oceanic variability such as El Niño-Southern Oscillation

35 (ENSO), Atlantic Multi-decadal Oscillation (AMO) and solar activity. In terms of current

36 climate conditions, our findings have important implications for developing drought-resistant

37 policies in communities on the fringes of Hindu Kush mountain Ranges in northern Pakistan.

38 Keywords: Tree rings, Growth-climate response, Drought variability, ENSO, dendroclimatology,

39 the broad-scale atmospheric-oceanic variability

40

41 **1. Introduction**

42   Numerous studies have shown that the intensity and frequency of drought events have

43 increased due to rapid climate warming (IPCC, 2013; Trenberth et al., 2014). The apparent

44 drought has had serious adverse effects on social, natural, and economic systems (Ficklin et al.,

45 2015; Yao and Chen, 2015; Tejedor et al., 2017; Yu et al., 2018). Global drought is considered to

46 be the most destructive climate disaster that has caused billions of dollars in worldwide loss (van

47 der Schrier et al., 2013; Lesk et al., 2016).

48   Pakistan has a semi-arid climate, and its agriculture economy is most vulnerable to drought

49 (Kazmi et al., 2015; Miyan, 2015). The long-term drought from 1998 to 2002 reduced

50 agricultural production, with the largest reduction in wheat, barley and sorghum (from 60% to

51 80%) (Ahmad et al., 2004). The northern Pakistan is considered to be the world's largest area of

52 irrigation network (Treydte et al., 2006). The production and life of local residents are strongly

53 dependent on monsoon precipitation brought by the mighty ocean and atmospheric circulation

54 system, including El Niño Southern Oscillation (ENSO), Atlantic Multi-decadal Oscillation

55 (AMO), Pacific Decadal Oscillation (PDO) and others (Treydte et al., 2006; Cook et al., 2010;

56 Miyan, 2015; Zhu et al., 2017). However, the current warming rate has changed the regional

57 hydrological conditions, leading to an unsustainable water supply (Hellmann et al., 2016; Wang

58 et al., 2017). It is not only critical for agricultural production but also leads to forest mortality,

59 vegetation loss (Martínez-Vilalta and Lloret, 2016) and increases the risk of wildfires (Turner et

60 al. 2015; Abatzoglou and Williams 2016). The degradation of grassland and loss of livestock

61 caused by drought eventually affect the lifestyle of nomadic peoples, especially in high-altitude

62 forested areas (Pepin et al., 2015; Shi et al., 2019).

63   The Hindu Kush Himalayan region (HKH) is the source of ten major rivers in Asia, which

64 provides water resources for one fifth of the world's population (Rasul, 2014; Bajracharya et al.,

65 2018). The region is particularly prone to drought, floods, avalanches and landslides, with more

66 than 1 billion people exposed to increasing frequency and serious risks of natural disasters

67 (Immerzeel et al., 2010; Immerzeel et al., 2013). The extent of climate change in this area is

68 significantly higher than the world average, which has seriously threatened the safety of life and

69 property, traffic and other infrastructure in the downstream and surrounding areas (Lutz et al.,

70 2014). Dry conditions are exacerbated by an increase in the frequency of heatwaves in recent

71 decades (Immerzeel et al., 2010; IPCC, 2013). The intensity and frequency of drought trend are

72 very complex in HKH, and there is no manifest measuring tool to compute how long the drought

73 period might persist. Climate uncertainty complicates the situation, for example, whether the

74 drought trend is increasing or decreasing (Chen et al., 2019). Most studies believe that the

75 wetting trend in HKH is going to increase in current decades (Treydte et al., 2006). However,

76 some extreme drought events in the region are very serious and persistent (Gaire et al., 2017).

77 Little has been done to examine the linkage between drought trend and large-scale ocean climate

78 drivers (Cook et al., 2003; Gaire et al., 2017). Besides in northern Pakistan, there is little research

79 on the dendroclimatology and instrumental climate records are inadequate in terms of quality and

80 longevity (Treydte et al., 2006; Khan et al., 2019). In high altitude, arid and semi-arid areas,

81 forest growth more sensitive to climate change, so dare need to understand more about the long-

82 term drought regimes of the past (Wang et al., 2008). Climate reconstruction is the best way to

83 understand long-term climate change and expand climate record to develop forest management

84 strategies. Researchers used multiple proxies, including ice cores, speleothems, lake sediments,

85 and historical documents and tree rings to reconstruct past short-term or long-term climate

86 change. In addition, tree rings were widely used in long-term paleoclimatic reconstructions and

87 forecasting future climate because of their accurate dating, high resolution, wide distribution,

88 easy access, long time series, and abundant environmental information recorded (Esper et al.,

89 2016; Zhang et al., 2015; Klippel et al., 2017; Shi et al., 2018; Chen et al., 2019)

90   In this study, we collected drought-sensitive tree-ring cores of *Cedrus deodar* from the upper

91 and lower HKH region of Pakistan. These tree rings have a good potential for dendroclimatic study

92 (Yadav, 2013). Then, the March-August Palmer Drought Sensitivity Index (PDSI) was

93 reconstructed for the past 424 years to examine the climatic variability and driving forces. To

94 verify its reliability, we compared our reconstructed PDSI with other available paleoclimatic

95 records (Treydte et al., 2006) near our research area. The intensity and drought mechanism in this

96 area were also discussed. This will be the first time that the drought index has been reconstructed

97 in northern Pakistan and is considered to be a baseline for more tree-ring reconstruction in

98 Pakistan.

99

100 **2 Material and Methods**

101 **2.1 Study area**

102 We conducted our research in the Chitral, Hindu-Kush (HK) Mountains of northern

103 Pakistan (35.36º N, 71.48º E, Fig. 1). Northern Pakistan is a subtropical monsoon climate.

104 Summer is dry and hot, spring is wet and warm, and in some high altitudes, it snows all the year-

105 round. March is the wettest month (with an average precipitation of 107 mm), while July or

106 August is the driest (with an average precipitation of 6.3 mm). July is the hottest month (mean

107 monthly temperature 36 ºC), and January is the coldest (mean monthly temperature -0.8 ºC) (Fig.

108 2). The soil at our sampling sites is acidic, with little variation among a stand of forest. Similarly,

109 the soil water holding capacity ranged from 47%±2.4% to 62%±4.6%, while the soil moisture

110 ranged from 28%±0.57% to 57%±0.49% (Khan et al., 2010). Chitral forest is mainly composed

111 of *Cedrus deodara, Juglans regia, Juniperus excelsa, Quercus incana, Q. diltata, Q. baloot* and

112 *Pinus wallichiana. C. deodara* was selected for sampling because of the high dendroclimatic

113 value (Khan et al., 2013).

Climate data such as monthly precipitation and temperature (1965-2016) were obtained

from the meteorological station of Chitral in northern Pakistan. PDSI downloaded from the

datasets of the nearest grid point (35.36º N, 71.48º E) through Climatic Research Unit (CRU

TS.3.22, 0.5º latitude × 0.5º longitude). The most common reliable period spanning from 1965 to

2016 was used (http://climexp.knmi.nl/) for dendroclimatic studies (Harris et al., 2014; Shekhar,

2015).

The Atlantic Multi-decadal Oscillation (AMO) index was downloaded from KNMI Climate

Explorer https://climexp.knmi.nl/data/iamo_hadsst.dat over the period 1890-2016. The

reconstructed June-August South Asia Summer Monsoon (JJA-SASM) data was downloaded

from Monsoon Asia Drought Atlas (MADA)

http://drought.memphis.edu/MADA/TimeSeriesDisplay.aspx over the period 1300-2005.

2.2 Tree rings collection and chronology development

Tree-ring cores collected in Chitral forest from *C. deodara* trees, located in the northern

area of Pakistan. To maintain the maximum climatic signals contained in tree rings, undisturbed

open canopy trees were selected. One core per tree at breast height (∼1.3 m above ground) was

sampled using a 5.15 mm diameter increment borer (Haglöf Sweden, Langsele, Sweden). In

addition, several ring-width series were also downloaded from the International Tree-Ring Data

Bank from the Bumburet forest and Zairat forest (https://www.ncdc.noaa.gov/paleo-search/)

collected in 2006 (Fig. 1).

All tree-ring samples were first glued than progressively mounted, dried, and polished

according to a set procedure (Fritts, 1976; Cook and Kairiukstis, 1990). The preceding calendar

136 year was assigned and properly cross-dated. False rings were identified by Skeleton-plot and

137 cross dated as mentioned in Stokes and Smiley (1968).

138   The cores were measured using the semi-automatic Velmex measuring system (Velmex,

139 Inc., Bloomfield, NY, USA) with an accuracy of 0.001 mm. The COFECHA program was then

140 used to check the accuracy of cross-dating and measurement (Holmes, 1983). All false one has

141 been modified and the cores that didn't match the master chronology were not used to develop

142 tree-ring chronology. For quality checks, the COFECHA 2002 program was used. (Holmes,

143 1998). The synthesized tree-ring width chronology (Fig. 3) was built by the program R (Zang

144 and Biondi, 2015). To preserve climate signals and avoid noise, appropriate detrending was

145 introduced. Biological trends of tree growth associated with tree age were conservatively

146 detrended by fitting negative exponential curves or linear lines (Fritts, 1976). The tree-ring

147 chronology was truncated where the expressed population signal (EPS) was large than 0.85,

148 which is a generally accepted standard for more reliable and potential climate signal results

149 (Wigley et al., 1984; Cook and Kairiukstis, 1990). The mean correlation between trees (Rbar),

150 means sensitivity (MS) and EPS was calculated to evaluate the quality of chronology (Fritts,

151 1976). Higher mean sensitivity and EPS were considered to be a strong response to climate

152 change (Cook and Kairiukstis, 1990).

153

154 **2.3 Statistical analysis**

155   Correlation analysis was conducted between tree-ring indexes (TRI) and monthly

156 temperature, precipitation, and PDSI (from previous June to current September, collected from

157 the nearby stations or downloaded from KNMI). Then, the PDSI was reconstructed according to

158 the relationship between TRI and climate variables. To test the validity and reliability of our

159 model, reconstruction was checked by the split-period calibration/verification methods subjected

160 to different statistical parameters, including reduction of error (RE), coefficient of efficiency

161 (CE), Pearson correlation coefficient (r), R-square (R^2), product mean test (PMT), sign test (ST)

162 and Durban-Watson test (DWT) (Fritts, 1976). PMT is used to test the level of consistency

163 between the actual and estimated values, taking into account the signs and magnitudes of

164 departures from the calibration average (Fritts, 1976). ST expresses the coherence between

165 reconstructed and instrumental climate data by calculating the number of coherence and

166 incoherence, which is often used in previous studies (Fritts, 1976; Cook et al., 2010). DWT is

167 used to calculate first-order autocorrelation or linear trend in regression residuals (Cook and

168 Pederson, 2011; Wiles et al., 2015). The RE and CE larger than zero were considered skills

169 (Fritts, 1976; Cook et al., 1999).

170 According to the reference of Chen et al. (2019), we defined the wet or dry years of our

171 reconstruction with the PDSI value greater than or less than the mean ±1 standard deviation. The

172 mean ±1 standard deviation is easy to calculate the dry and wet years, which has been observed

173 in different tree-ring PDSI reconstructions (Wang et al., 2008; Chen et al., 2019). We assessed

174 the dry and wet periods for many years based on strength and intensity.

175 Although there were few reconstructions in our study area, we compared our reconstruction

176 with other available drought reconstructions near the study area (Treydte et al., 2006). The multi-

177 taper method (MTM) was used for spectral analysis, and the Wavelet analysis was used to

178 determine the statistical significance of band-limited signals embedded in red noise by providing

179 very high-resolution spectral estimates that eventually give best possible option against leakage.

180 To identify the local climate change cycle, the background spectrum was used (Mann and Lees,

181 1996).

182

3 Results

3.1 Main climate limiting factors for Cedrus deodar

The statistical parameters of the tree-ring chronologies, including MS (0.16), Rbar (0.59), and EPS (0.94) indicated that there were enough common signals in our sampled cores, and our chronology is suitable for dendroclimatic study. According to the threshold of EPS (EPS > 0.85), 1593-2016 was selected as the reconstruction period to truncate the period 1537-1593 of the chronology (Fig. 3).

The TRI was significantly positively correlated with monthly PDSI ($p<0.01$) (Fig. 4a). However, the TRI was positively correlated with the precipitation in October of the previous year and February-May of the current year, and negatively correlated with the precipitation in September of the previous year ($p<0.001$). The TRI was significantly positively ($p < 0.001$) with the minimum temperature in September and December of the previous year and January and February of the current year (Fig. 4b). Similarly, the TRI was significantly negatively ($p < 0.001$) correlated the maximum temperature in January, October and December of the previous year and February-June of the current year. The TRI was only significantly positively correlated the maximum temperature in September (Fig. 4b).

3.2 Reconstruction of the past drought variation in northern Pakistan

The correlation between and TRI was the highest from March to August, indicating that the growth of *C. deodara* was most strongly affected by the drought before and during the growing season. Based on the above correlation analysis results, the March-August PDSI was the most suitable for seasonal reconstruction. The linear regression model between TRI and mean March-

205 August PDSI for the calibration period from 1960 to 2016 was significant (F=52.4, p <0.001,

206 adjusted R^2 = 0.49, r =0.70). The regression model was:

207   Y= 5.1879x - 5.676

208   Where Y is the mean March-August PDSI and x is the tree-ring index.

209   The split calibration-verification test showed that the variance explained was higher during

210 the two calibration periods (1960-1988 and 1989-2016). For the calibration period (1960-2016),

211 the reconstruction accounted for 39.2% of the scPDSI variation (37.6 after accounting for the

212 loss of degrees of freedom). Statistics of R, R^2, ST, and PMT are all significant at p <0.05,

213 indicating that the model was reliable (Table 1). The RE and CE has a theoretical range of -∞ to

214 +1, but the benchmark for determining skill is the calibration and verification period mean.

215 Therefore, a RE >0 and CE >0 indicates reconstruction skill in excess of climatology (Cook et

216 al., 1999). Here, the most rigorous RE and CE tests in the verification period were all positive.

217 Hence, these results made the model more obvious and robust in PDSI reconstruction.

218   The instrumental and reconstructed scPDSIs of the Hindu Kush Mountains had similar

219 trends and parallel calibrations during short- and long-time scales in the 20th century (Fig. 5).

220 However, the reconstructed scPDSI did not fully capture the magnitude of extremely dry or wet

221 conditions.

222

223 **3.3 The drought regime in the Chitral Mountain, northern Pakistan for the past 424 years**

224   Fig. 5 showed the dry and wet years of the past 424 years (1593-2016) in the Chitral

225 Mountain in northern Pakistan. The dry periods were recorded in 1593-1598, 1602-1608, 1631-

226 1645, 1647-1660, 1756-1765, 1785-1800, 1870-1878, 1917-1923, and 1981-1995. Similarly, the

227 wet periods were recorded in 1663-1675, 1687-1708, 1771-1173, 1806-1814, 1844-1852, 1932-

228 1935, 1965-1969, and 1996-2003.

229   To verify the accuracy and reliability of our reconstruction, we compared our results with

230 the nearby precipitation reconstruction of Treydte et al. (2006) (Fig. 6). In the reconstruction of

231 Treydte et al. (2006), the high and low raw $\delta^{18}O$ value represents dry and wet conditions,

232 respectively, just opposite to the PDSI index. In most periods, our PDSI reconstruction and the

233 precipitation reconstruction of Treydte et al. (2006) showed good consistency (Fig. 6). However,

234 in some periods, they also showed inconsistent or even opposite changes in drought

235 reconstruction. For example, in 1865-1900, the reconstruction of Treydte et al. (2006) was very

236 wet, while our reconstruction was normal. In periods 1800-1810 and 1694-1702, the

237 reconstruction of Treydte et al. (2006) was very dry, but our reconstruction was wet (Fig. 6).

238   Spectral analysis showed that the historical PDSI changes in the Hindukush Mountains

239 showing several significant (95% or 99% confidence level) with periods at 33-38 (99%), 16.8

240 (99%), 2-3 (99%) years, corresponding to significant periodic peaks (Fig. 7).

241   The spatial correlation analysis between our reconstructed and actual PDSI from May to

242 August shows that our drought reconstruction is a good regional representative (Fig. 8). This

243 shows that our reconstruction is reliable and can reflect the drought situation in the region. In

244 addition, the PDSI of low-frequency (the 31-year moving average) reconstruction had good

245 consistency with AMO ($r = 0.53$, $p < 0.001$, 1890-2001) and SASM ($r = 0.35$, $p < 0.001$, 1608-

246 1990), which indicated that these are the potential factors affecting the drought pattern in the

247 region.

248

249 **4 Discussion**

4.1 Drought variation in Chitral HinduKush Range of Pakistan

The growth-climate relationship revealed the positive and negative influence of precipitation and summer temperature on growth. It means that water availability (PDSI) is the main limiting factor affecting the growth of *C. deodara*. Singh et al. (2006) reported that the previous October precipitation limited the growth of *C. deodara*, while Ahmed et al. (2011) found no such effect. Except for last August, November, and current September, maximum temperature has a negative impact on the growth of *C. deodara*, while the minimum temperature does not. These results suggest that moisture conditions in April-July are critical to the growth of *C. deodar* in the study area (Borgaonkar et al., 1996; Hussain et al., 2007; Khan et al., 2013). Remarkably, Chitral does not receive monsoon rains. That's why it is hard to understand how trees respond to different moisture trends.

Here we developed a 467-year (1550-2017) of tree ring chronology of *C. deodara,* and reconstructed the 424-year (1593-2016) drought variability of the Chitral Hindukush Range in northern Pakistan. The point years (narrow rings), 2002, 2001, 2000, 1999, 1985, 1971, 1962, 1952, 1945, 1921, 1917, 1902 and 1892, were recorded in our tree-ring record. The narrow ring formation occurs when extreme drought stress reduces cell division (Fritts et al., 1976; Shi et al., 2014). Therefore, the narrow rings are also consistent with the extreme drought years. Among them, 2001, 1999, 1952, and 1921 were identified by previous studies (Esper et al., 2003; Ahmed et al. 2010; Zafar et al., 2010; Khan et al., 2013; He et al., 2018). Sigdel and Ikeda (2010) reported that droughts occurred in 1974, 1977, 1985, 1993, and the winter of 2001 and the summers of 1977, 1982, 1991, and 1992. Our PDSI reconstruction fully captured the widespread drought in Pakistan, Afghanistan, and Tajikistan in 1970-1971 (Yu et al., 2014). The above drought has disrupted the people's daily life, leading to food and water shortages and livestock

273 losses in high altitude areas (Yadav, 2011; Yadav and Bhutiyani, 2013; Yadav et al., 2017). This

274 drought may also be due to the failure of Western disturbance precipitation (Hoerling et al.,

275 2003).

276   In Fig. 5, the mean of our reconstructed PDSI is below zero. There are two possible reasons

277 for this phenomenon. First, tree growth is more sensitive to drying than to wetting. As a result,

278 more drought information is recorded in ring widths. This leads to a drier (less than zero) PDSI

279 reconstructed with tree rings. This phenomenon exists in many tree-ring PDSI reconstructions

280 (Hartl-Meier et al., 2017; Wang et al., 2008). Second, the period (1960-2016) used to reconstruct

281 the equation is relatively dry. This cause the mean of the reconstruction equation to be lower

282 than zero (dry), resulting in lower values for the whole reconstructions. Therefore, when

283 applying the PDSI data reconstructed by tree rings, its relative value is relatively reliable, and the

284 absolute value data can only be used after adjustment. The adjustment method of the absolute

285 value needs to be further studied.

286   Our reconstruction also captured a range of climate changes mentioned in other studies

287 (Ahmad et al., 2004; Yu et al., 2014; Chen et al. 2019; Gaire et al., 2019). Our dry periods

288 (1981-1987, 1870-1875 to 1761-1764) were consistent with the results of Chen et al. (2019). The

289 dry period 1645-1631 also reported in tree-ring based drought variability of Silk Road (Yu et al.,

290 2014). Most notably, three mega drought events in Asian history (Yadav, 2013; Panthi et al.,

291 2017; Gaire et al., 2019), namely, the Strange Parallels drought (1756-1768), the East India

292 drought (1790-1796) and late Victorian Great Drought (1876 to 1878) was clearly recorded in

293 our reconstructed PDSI. Based on the above results, drought changes in Northern Pakistan and

294 the central Himalayas are closely related to large-scale ocean-atmospheric circulation and

295 synchronous in western Asia (Gaire et al., 2019). The driest period of 1917-1921 of our

296 reconstruction, followed by another dry period 1784-1802, coincided with the eruption of Laki

297 volcano (Iceland) in 1783. This could mean that widespread drought on the continent could be

298 linked to volcanic eruptions (Chen et al., 2019). Interestingly, the wet period of 1995-2016 was

299 very consistent with those of Yadav et al. (2017). These results suggested that the long-term

300 continuous wets in 31 years of the past 576 years (1984-2014) may have increased the mass of

301 glaciers in the northwest Himalaya and Karakoram (Cannon et al., 2014). The devastating floods

302 of July 2010 were also captured by our reconstruction, affecting about a fifth of Pakistan (20

303 million peoples) (Yaqub et al., 2015). Therefore, we speculate that the size of the Hindukush

304 glacier and the mass of glaciers near our study areas will continue to increase if it continues to

305 get wet.

306   Our PDSI reconstruction and the precipitation reconstruction of Treydte et al. (2006)

307 showed a strong consistency (Fig. 6), which proves that our reconstruction is reliable. The

308 inconsistency between them in some periods may be because the PDSI is affected by temperature

309 and may not be completely consistent with precipitation (Li et al., 2015). The inconsistency

310 between the reconstruction of ring width and oxygen isotope in some periods may also be due to

311 the different response of radial growth and isotope to disturbance (McDowell et al., 2002). In

312 addition, the lack of consistency between different data sets or regions may be due to the

313 dominance of internal climate variability over the impact of natural exogenous forcing conditions

314 on multi-decadal timescales (Bothe et al., 2019).

315

316 **4.2 The linkage of drought variation with the ocean oscillations**

317   The results of wavelet and MTM analysis indicated that the low and high-frequency periods

318 of drought in northern Pakistan may teleconnection with both large-small scale climate

319 oscillation (Fig. 7). The spatial correlation exhibited the significant similarity of El Niño-

320 Southern Oscillation (ENSO) in the region (Fig. 8). The intensity of India monsoon in this area

321 was modulated by ENSO patterns. The high frequency of drought cycle (2.1-3.3 years) may be

322 related to the ENSO (van Oldenborgh and Burgers, 2005). Khan et al. (2014) showed that most

323 of our study area is covered by monsoon shadow, but the Asian monsoon showed an overall

324 weak trend in recent decades (Wang and Ding, 2006; Ding et al., 2008). Therefore, the increase

325 of regional precipitation may be linked to the ENSO. Previous studies (Wang et al., 2006; Palmer

326 et al., 2015; Shi et al., 2018; Chen et al., 2019) have confirmed that ENSO is an important factor

327 in regulating the hydrological conditions related to the AMO. In the past, sever famine and

328 drought occurred simultaneously with the warm phase of ENSO, and these events were related to

329 the failure of Indian Summer Monsoon (Shi et al., 2014).

330 The middle-frequency cycle (16 years) may be related to the solar cycle, which is similar to

331 other studies in South Asia (Panthi et al., 2017; Shekhar et al., 2018; Chen et al., 2019). Solar

332 activity may affect climate fluctuations in the Chitral, Hindukush ranges, northern Pakistan

333 (Gaire et al., 2017). The low-frequency (36-38 years) may be caused by the Atlantic Multi-

334 decadal Oscillation (AMO), which is the anomalies of sea surface temperatures (SST) in the

335 North Atlantic basin. Previous studies have shown that the AMO may alter drought or

336 precipitation patterns in North America (Mccabe et al., 2004; Nigam et al., 2011) and Europe

337 (Vicente-Serrano and López-Moreno, 2008). Although our study area is far from the Atlantic

338 Ocean, it may also be affected by AMO (Lu et al., 2006; Wang et al., 2011; Yadav, 2013). Lu et

339 al. (2006) found that the SST anomalies in the North Atlantic (such as AMO) can affect the

340 Asian summer monsoon. Goswami et al. (2006) reported the mechanism for the AMO influence

341 on the Indian monsoon precipitation. The warm AMO appears to cause a late withdrawal of the

Indian monsoon through strengthening the meridional gradient of tropospheric temperature in autumn (Goswami et al., 2006; Lu et al., 2006). Yadav (2013) suggested that the role of AMO in modulating winter droughts over the western Himalaya through the tropical Pacific Ocean. Wang et al. (2009) pointed out that the AMO heat the Eurasian middle and upper troposphere in all four seasons, resulting in weakened Asian winter monsoons but enhanced summer monsoons. This is consistent with the findings that the AMO affecting climate in China, which is made possible by the Atlantic-Eurasia wave train from the North Atlantic and increased due to global warming (Qian et al., 2014). Further work is still needed to unravel the links between the Pacific and Atlantic Oceans and how the two are coupled through the atmosphere and oceans to affect drought in Asia.

Dimri (2006) found that the precipitation surplus in winter from 1958 to 1997 was related to the significant heat loss in the northern Arabian Sea, mainly due to intensification of water vapor flow in the west and the enhancement of evaporation. As a result, large-scale changes in Atlantic temperature could also regulate western Asia climate. Our result was supported by other dendroclimatic studies (Sano et al., 2005; Chen et al., 2019). Precipitation in Mediterranean, Black sea (Hatwar et al., 2005; Giesche et al., 2019), and parts of northern Pakistan showed an upward trend from 1980 to 2010, but the precipitation in the Chitral Mountains received from Winter Indian Monsoon (WID) (December-March) and the rain shadows in summer (Khan et al., 2013). Predicting different climate cycle patterns is not easy. Besides, the flow of the Upper Indus Basin (UIB) depends on changes in the Ablation air mass (Rashid et al., 2018; Rao et al., 2018), so small changes in the Ablation mass may eventually lead to changes in water quality and quantity. The UIB is considered as a water tower in the plain (Immerzeel et al., 2010), so the

364   Hindukush Mountains are particularly important for extending the proxy network to improve

365   understanding of different climatic behaviors.

366   Due to reconstruction indices, species, geographical differences and other reasons, it does

367   not remain the same with the whole period. The drought regimes in Hindukush ranges in

368   northern Pakistan may be linked to regional, local, and global climate change. We only studied

369   the response of *C. deodara* to different climate change in the Chitral region, northern Pakistan.

370   Therefore, we suggest further high-resolution and well-dated record are needed to augment

371   dendroclimatic network in the region.

372

5 Conclusion

374   Based on the significance of the tree-ring width of *C. deodara*, we developed a 467-years

375   chronology (1550-2017). Considering that EPS threshold is greater than 0.85 (> 5 trees), we

376   reconstructed the current March-August PDSI from 1593 to 2016. Our reconstruction captured

377   different drought changes in different time scale in the Chitral, Hindukush Mountain, Pakistan,

378   which falls in the Indus civilization. Several studies have shown that the Indus civilization

379   changed dramatically in history because of its unpleasant climate. Three historic mega drought

380   events, the Strange Parallel Droughts (1756-1768) the East Indian Drought (1790-1796) and late

381   Victorian Great Drought (1876-1878) were captured by our reconstructed PDSI. These large

382   scales and small droughts may be caused by cold or hot climate. Our results are consistent with

383   other dendroclimatic records, which further support the feasibility of our reconstruction. Besides,

384   due to a different climate change patterns in the region, we suggested extending the different

385   proxy networks to understand the remote teleconnection across the continent on the multi-

386   decadal to centennial timescales to meet future climate challenges.

387

Acknowledgments

This research was supported by the Key Project of the China National Key Research and Development Program (2016YFA0600800), the Fundamental Research Funds for the Central Universities (2572019CP15 and 2572017DG02), the Open Grant for Eco-meteorological Innovation Laboratory in northeast China, China Meteorological Administration (stqx2018zd02), and the Chinese Scholarship Council. We appreciate the staff of the International Office, Northeast Forestry University for their excellent services. We thank Dr. Muhmmad Usman, Mr. Shahid Humayun Mirza and Dr. Nasrullah Khan for their communications in revising the manuscript. We also appreciate Mr. Muhmmad Arif, Sher Bahder, Wali Ullah and Mushtaq Ahmad for their great help in the fieldwork.

Data availability

The reconstructed PDSI can be obtained from the supplementary file of this paper. The tree-ring width used in this paper can be download from the International Tree-ring Data Bank.

Author contributions

Xiaochun Wang and Sarir Ahmad initiated this idea. Sarir Ahmad and Sami Ullah collected samples in the field. Liangjun Zhu and Sumaira Yasmeen crossdated and measured the samples. Sarir Ahmad and Xiaochun Wang wrote the manuscript. Liangjun Zhu, Yuandong Zhang, Zongshan Li and Shijie Han revised the manuscript.

Competing interest

410   The authors declare that they have no conflict of interest.

411

412   **References**

413   Abatzoglou, J. T., and Williams, A. P.: Impact of anthropogenic climate change on wildfire

414   across western US forests, Proceedings of the National Academy of Sciences, 113, 11770-

415   11775, 2016.

416   Ahmed, M., Khan, N., and Wahab, M.: Climate response function analysis of *Abies pindrow*

417   (Royle) Spach. preliminary results, Pakistan Journal of Botany, 42, 165-171, 2010.

418   Ahmed, M., Shaukat, S. S., and Siddiqui, M. F.: A multivariate analysis of the vegetation of

419   *Cedrus deodara* forests in Hindu Kush and Himalayan ranges of Pakistan: evaluating the

420   structure and dynamics, Turkish Journal of Botany, 35, 419-438, 2011.

421   Ahmad, S., Hussain, Z., Qureshi, A. S., Majeed, R., and Saleem, M.: Drought mitigation in

422   Pakistan: current status and options for future strategies, Working Paper 85. Colombo, Sri

423   Lanka: International Water Management Institute, 2004.

424   Bajracharya, A. R., Bajracharya, S. R., Shrestha, A. B., and Maharjan, S. B.: Climate change

425   impact assessment on the hydrological regime of the Kaligandaki Basin, Nepal, Science of

426   the Total Environment, 625, 837-848, 2018.

427   Borgaonkar, H., Pant, G., and Rupa Kumar, K.: Ring-width variations in *Cedrus deodara* and its

428   climatic response over the western Himalaya, International Journal of Climatology: A

429   Journal of the Royal Meteorological Society, 16, 1409-1422, 1996.

430   Bothe, O., Wagner, S., and Zorita, E.: Inconsistencies between observed, reconstructed, and

431   simultaed precipitation indices for England since the year 1650 CE, Climate of the Past, 15,

432   307-334, 2019.

433 Cannon, F., Carvalho, L. M. V., Jones, C., and Bookhagen, B.: Multi-annual variations in winter

434   westerly disturbance activity affecting the Himalaya. Climate Dynamics, 44, 441-455, 2015.

435 Chen, F., Zhang, T., Seim, A., Yu, S., Zhang, R., Linderholm, H. W., Kobuliev, Z. V., Ahmadov,

436   A., and Kodirov, A.: Juniper tree-ring data from the Kuramin Range (northern Tajikistan),

437   reveals changing summer drought signals in western Central Asia. Forests, 10(6), 505,

438   2019.

439 Cook, E. R., Anchukaitis, K. J., Buckley, B. M., D'Arrigo, R. D., Jacoby, G. C., and Wright, W.

440   E.: Asian monsoon failure and megadrought during the last millennium, Science, 328, 486-

441   489, 2010.

442 Cook, E. R., Meko, D. M., Stahle, D. W., and Cleaveland, M. K.: Drough reconstruction for the

443   continental United States, Journal of Climate, 12, 1145-1162, 1999.

444 Cook, E. R., and Pederson, N.: Uncertainty, emergence, and statistics in dendrochronology, in:

445   Hughes, M. K., Swetnam, T. W., and Diaz, H. F., Dendroclimatology, Springer, Dordrecht,

446   USA, 77-112, 2011.

447 Cook, E. R., and Kairiukstis, L. A.: Methods of dendrochronology: applications in the

448   environmental sciences, Kuluwer Academic Publishers, Dordrecht, USA, 1990.

449 Cook, E. R., Krusic, P. J., and Jones, P. D.: Dendroclimatic signals in long tree-ring chronologies

450   from the Himalayas of Nepal, International Journal of Climatology, 23, 707-732, 2003.

451 Dimri, A.: Surface and upper air fields during extreme winter precipitation over the western

452   Himalayas, Pure and Applied Geophysics, 163, 1679-1698, 2006.

453 Esper, J., Shiyatov, S., Mazepa, V., Wilson, R., Graybill, D., and Funkhouser, G.: Temperature-

454   sensitive Tien Shan tree ring chronologies show multi-centennial growth trends, Climate

455   Dynamics, 21, 699-706, 2003.

456 Esper, J., Krusic, P. J., Ljungqvist, F. C., Luterbacher, J., Carrer, M., Cook, E., Davi, N. K.,

457   Hartl-Meier, C., Kirdyanov, A., and Konter, O.: Ranking of tree-ring based temperature

458   reconstructions of the past millennium, Quaternary Science Reviews, 145, 134-151, 2016.

459 Ficklin, D. L., Maxwell, J. T., Letsinger, S. L., and Gholizadeh, H.: A climatic deconstruction of

460   recent drought trends in the United States, Environmental Research Letters, 10, 044009,

461   2015.

462 Fritts, H. C.: Tree rings and climate. Academic Press, New York, USA, 1976.

463 Gaire, N. P., Bhuju, D. R., Koirala, M., Shah, S. K., Carrer, M., and Timilsena, R.: Tree-ring

464   based spring precipitation reconstruction in western Nepal Himalaya since AD 1840,

465   Dendrochronologia, 42, 21-30, 2017.

466 Gaire, N. P., Dhakal, Y. R., Shah, S. K., Fan, Z.-X., Bräuning, A., Thapa, U. K., Bhandari, S.,

467   Aryal, S., and Bhuju, D. R.: Drought (scPDSI) reconstruction of trans-himalayan region of

468   central himalaya using *Pinus wallichiana* tree-rings, Palaeogeography, Palaeoclimatology,

469   Palaeoecology, 514, 251-264, 2019.

470 Giesche, A., Staubwasser, M., Petrie, C. A., and Hodell, D. A.: Indian winter and summer

471   monsoon strength over the 4.2 ka BP event in foraminifer isotope records from the Indus

472   River delta in the Arabian Sea, Climate of the Past, 15, 73-90, 2019.

473 Goswami, B.N., Madhusoodanan, M.S., Neema, C.P., Sengupta, D.: A physical mechanism for

474   North Atlantic SST influence on the Indian summer monsoon, Geophysical Research

475   Letters, 33, L02706, 2006.

476 Harris, I., Jones, P. D., Osborn, T. J., and Lister, D. H.: Updated high-resolution grids of monthly

477   climatic observations–the CRU TS3. 10 Dataset, International Journal of Climatology, 34,

478   623-642, 2014.

479   Hartl-Meier, C., Büntgen, U., Smerdon, J. E., Zorita, E., Krusic, P. J., Ljungqvist, F. C.,

480   Schneider, L., and Esper, J.: Temperature covariance in tree ring reconstructions and model

481   simulations over the past millennium, Geophysical Research Letters, 44, 9458-9469, 2017.

482   Hatwar, H., Yadav, B., and Rao, Y. R.: Prediction of western disturbances and associated

483   weather over Western Himalayas, Current Science, 88, 913-920, 2005.

484   He, M., Bräuning, A., Grießinger, J., Hochreuther, P., and Wernicke, J.: May–June drought

485   reconstruction over the past 821 years on the south-central Tibetan Plateau derived from

486   tree-ring width series, Dendrochronologia, 47, 48-57, 2018.

487   Hellmann, L., Agafonov, L., Ljungqvist, F. C., Churakova, O., Düthorn, E., Esper, J., Hülsmann,

488   L., Kirdyanov, A. V., Moiseev, P., and Myglan, V. S.: Diverse growth trends and climate

489   responses across Eurasia's boreal forest, Environmental Research Letters, 11, 074021,

490   2016.

491   Hoerling, M., and Kumar, A.: The perfect ocean for drought, Science, 299, 691-694, 2003.

492   Holmes, R.: Computer assisted quality control, Tree-ring Bulletin, 43, 69-78, 1983.

493   Hussain, F., Shah, S. M., and Sher, H.: Traditional resource evaluation of some plants of Mastuj,

494   District Chitral, Pakistan, Pakistan Journal of Botany, 39, 339-354, 2007.

495   Immerzeel, W. W., P ellicciotti, F., and Bierkens, M. F. P.: Rising river flows throughout the

496   twenty-first century in two Himalayan glacierized watersheds, Nature Geoscience, 6, 742-

497   745, 2013.

498   Immerzeel, W. W., van Beek, L. P., and Bierkens, M. F.: Climate change will affect the Asian

499   water towers, Science, 328, 1382-1385, 2010.

500   IPCC., Stocker, T.F., Qin, D., Plattner, G.K., Tignor, M., Allen, S.K., Boschung, J., Nauels, A.,

501   Xia, Y., Bex, V., Midgley, P.M. (Eds.), The Physical Science Basis.: Climate change,

Contribution of Working Group I to the Fifth Assessment Report of the

Intergovernmental Panel on Climate Change. Cambridge University Press, Cambridge

and New York. 2013

Kazmi, D. H., Li, J., Rasul, G., Tong, J., Ali, G., Cheema, S. B., Liu, L., Gemmer, M., and

Fischer, T.: Statistical downscaling and future scenario generation of temperatures for

Pakistan region, Theoretical and Applied Climatology, 120, 341-350, 2015.

Khan, N., Ahmed, M., Wahab, M., and Ajaib, M.: Phytosociology, structure and physiochemical

analysis of soil in *Quercus baloot* Griff, forest fistrict Chitral Pakistan, Pakistan Journal of

Botany, 42, 2429-2441, 2010.

Khan, N., Ahmed, M., and Shaukat, S.: Climatic signal in tree-ring chronologies of *Cedrus*

deodara from Chitral HinduKush Range of Pakistan, Geochronometria, 40, 195-207, 2013.

Klippel, L., Krusic, P. J., Brandes, R., Hartl-Meier, C., Trouet, V., Meko, M., and Esper, J.:

High-elevation inter-site differences in Mount Smolikas tree-ring width data,

Dendrochronologia, 44, 164-173, 2017.

Lesk, C., Rowhani, P., and Ramankutty, N.: Influence of extreme weather disasters on global

crop rpoduction, Nature, 529, 84-87, 2016.

Li, Q., Liu, Y., Song, H., Yang, Y., and Zhao, B.: Divergence of tree-ring-based drought

reconstruction between the individual sampling site and the Monsoon Asia Drought Atlas:

an example from Guancen Mountain, Science Bulletin, 60(19), 1688-1697.

Lu, R., Dong, B., Ding, H.: Impact of the Atlantic Multidecadal Oscillation on the Asian summer

monsoon, Geophysical Research Letters, 33, 194-199, 2006.

523 Lutz, A. F., Immerzeel, W. W., Shrestha, A. B., and Bierkens, M. F. P.: Consistent increase in

524   high Asia's runoff due to increasing glacier melt and precipitation. Nature Climate Change,

525   4, 587, 2014.

526 McDowell, N., Brooks, J. R., Fitzgerald, S., and Bond, B. J.: Carbon isotope discrimination and

527   growth response to stand density reductions in old *Pinus ponderosa* trees. Presented at 3rd

528   International Conference on Applications of Stable isotope Techniques to Ecological

529   Studies, Flagstaff, AZ, April 29-May 1, 2002.

530 Mann, M. E., and Lees, J. M.: Robust estimation of background noise and signal detection in

531   climatic time series, Climatic Change, 33, 409-445, 1996.

532 Martínez-Vilalta, J., and Lloret, F.: Drought-induced vegetation shifts in terrestrial ecosystems:

533   the key role of regeneration dynamics, Global and Planetary Change, 144, 94-108, 2016.

534 Mccabe, G.J., Palecki, M.A., Betancourt, J.L.: Pacific and Atlantic Ocean influences on

535   multidecadal drought frequency in the United States, Proceedings of the National Academy

536   of Sciences of the United States of America 101, 4136-4141, 2004.

537 Miyan, M. A.: Droughts in Asian least developed countries: vulnerability and sustainability,

538   Weather and Climate Extremes, 7, 8-23, 2015.

539 Nigam, S., Guan, B., Ruiz-Barradas, A.: Key role of the Atlantic Multidecadal Oscillation in

540   20th century drought and wet periods over the Great Plains, Geophysical Research Letters,

541   38, 239-255, 2011.

542 Palmer, J. G., Cook, E. R., Turney, C. S., Allen, K., Fenwick, P., Cook, B. I., O'Donnell, A.,

543   Lough, J., Grierson, P., and Baker, P.: Drought variability in the eastern Australia and New

544   Zealand summer drought atlas (ANZDA, CE 1500–2012) modulated by the Interdecadal

545   Pacific Oscillation, Environmental Research Letters, 10, 124002, 2015.

Panthi, S., Bräuning, A., Zhou, Z.-K., and Fan, Z.-X.: Tree rings reveal recent intensified spring drought in the central Himalaya, Nepal, Global and Planetary Change, 157, 26-34, 2017.

Pepin, N., Bradley, R., Diaz, H., Baraer, M., Caceres, E., Forsythe, N., Fowler, H., Greenwood G, Hashmi, M. Z., Liu, X. D., Miller, J. R., Ning, L., Ohmura, A., Palazzi, E., Rangwala, I., Schöner, W., Severskiy, I., Shahgedanova, M., Wang, M. B., Williamson, S. N., and Yang D. Q.: Elevation-dependent warming in mountain regions of the world, Nature Climate Change, 5, 424-430, 2015.

Qian, C., Yu, J., Chen, G.: Decadal summer drought frequency in China: the increasing influence of the Atlantic Multi-decadal Oscillation, Environmental Research Letters 9, 124004, 2014.

Rao, M. P., Cook, E. R., Cook, B. I., Palmer, J. G., Uriarte, M., Devineni, N., Lall, U., D'Arrigo, R. D., Woodhouse, C. A., and Ahmed, M.: Six centuries of upper Indus Basin streamflow variability and its climatic drivers, Water Resources Research, 54, 5687-5701, 2018.

Rashid, M. U., Latif, A., and Azmat, M.: Optimizing irrigation deficit of multipurpose Cascade reservoirs, Water Resources Management, 32, 1675-1687, 2018.

Rasul, G.: Food, water, and energy security in South Asia: A nexus perspective from the Hindu Kush Himalayan region, Environmental Science & Policy, 39, 35-48, 2014.

Sano, M., Furuta, F., Kobayashi, O., and Sweda, T.: Temperature variations since the mid-18th century for western Nepal, as reconstructed from tree-ring width and density of Abies spectabilis, Dendrochronologia, 23, 83-92, 2005.

Shekhar, M.: Application of multi proxy tree ring parameters in the reconstruction of climate vis-à-vis glacial fluctuations from the eastern Himalaya, University of Lucknow, Lucknow, India, 2015.

Shekhar, M., Pal, A. K., Bhattacharyya, A., Ranhotra, P. S., and Roy, I.: Tree-ring based
    reconstruction of winter drought since 1767 CE from Uttarkashi, Western Himalaya,
    Quaternary International, 479, 58-69, 2018.

Shi, F., Li, J., and Wilson, R. J.: A tree-ring reconstruction of the South Asian summer monsoon
    index over the past millennium, Scientific Reports, 4, 6739, 2014.

Shi, C., Shen, M., Wu, X., Cheng, X., Li, X., Fan, T., Li, Z., Zhang, Y., Fan, Z., and Shi, F.:
    Growth response of alpine treeline forests to a warmer and drier climate on the southeastern
    Tibetan Plateau, Agricultural and Forest Meteorology, 264, 73-79, 2019.

Shi, H., Wang, B., Cook, E. R., Liu, J., and Liu, F.: Asian summer precipitation over the past 544
    years reconstructed by merging tree rings and historical documentary records, Journal of
    Climate, 31, 7845-7861, 2018.

Sigdel, M., and Ikeda, M.: Spatial and temporal analysis of drought in Nepal using standardized
    precipitation index and its relationship with climate indices, Journal of Hydrology and
    Meteorology, 7, 59-74, 2010.

Singh, J., Park, W. K., and Yadav, R. R.: Tree-ring-based hydrological records for western
    Himalaya, India, since AD 1560, Climate Dynamics, 26, 295-303, 2006.

Stokes, M. A., and Smiley, T. L.: An introduction to tree-ring dating, University of Arizona
    Press, Tucson, USA, 1968.

Sun, C., and Liu, Y.: Tree-ring-based drought variability in the eastern region of the Silk Road
    and its linkages to the Pacific Ocean, Ecological Indicators, 96, 421-429, 2019.

Tejedor, E., Saz, M., Esper, J., Cuadrat, J., and de Luis, M.: Summer drought reconstruction in
    northeastern Spain inferred from a tree ring latewood network since 1734, Geophysical
    Research Letters, 44, 8492-8500, 2017.

Trenberth, K. E., Dai, A., van der Schrier, G., Jones, P. D., Barichivich, J., Briffa, K. R., and Sheffield, J.: Global warming and changes in drought, Nature Climate Change, 4, 17-22, 2014.

Treydte, K. S., Schleser, G. H., Helle, G., Frank, D. C., Winiger, M., Haug, G. H., and Esper, J.: The twentieth century was the wettest period in northern Pakistan over the past millennium. Nature, 440, 1179-1182, 2006.

Turner, D. P., Conklin, D. R., and Bolte, J. P.: Projected climate change impacts on forest land cover and land use over the Willamette River Basin, Oregon, USA, Climatic Change, 133, 335-348, 2015.

van der Schrier, G., Barichivich, J., Briffa, K., and Jones, P.: A scPDSI-based global data set of dry and wet spells for 1901–2009, Journal of Geophysical Research: Atmospheres, 118, 4025-4048, 2013.

van Oldenborgh, G. J., and Burgers, G.: Searching for decadal variations in ENSO precipitation teleconnections, Geophysical Research Letters, 32, L15701, 2005.

Vicente-Serrano, S.M., López-Moreno, J.I.: Nonstationary influence of the North Atlantic Oscillation on European precipitation. Journal of Geophysical Research-Atmospheres, 113, D20120, 2008.

Wang, B., Ding, Q., and Jhun, J. G.: Trends in Seoul (1778–2004) summer precipitation, Geophysical Research Letters, 33, L15803, 2006.

Wang, H., Chen, F., Ermenbaev, B., and Satylkanov, R.: Comparison of drought-sensitive tree-ring records from the Tien Shan of Kyrgyzstan and Xinjiang (China) during the last six centuries, Advances in Climate Change Research, 8, 18-25, 2017.

Wang, X., Brown, P.M., Zhang, Y., Song, L.: Imprint of the Atlantic multidecadal oscillation on tree-ring widths in northeastern Asia since 1568, PlOS ONE, 6, e22740, 2011.

Wang, X., Zhang, Q., Ma, K., and Xiao, S.: A tree-ring record of 500-year dry-wet changes in northern Tibet, China, Holocene, 18, 579-588, 2008.

Wang, Y., Li, S., Luo, D.: Seasonal response of Asian monsoonal climate to the Atlantic Mutidecadal Oscillation, Journal of Geophysical Research-Atmospheres 114, D02112, 2009.

Wigley, T. M., Briffa, K. R., and Jones, P. D.: On the average value of correlated time series, with applications in dendroclimatology and hydrometeorology, Journal of climate and Applied Meteorology, 23, 201-213, 1984.

Wiles, G. C., Solomina, O., D'Arrigo, R., Anchukaitis, K. J., Gensiarovsky, Y. V., and Wiesenberg, N.: Reconstructed summer temperatures over the last 400 years based on larch ring widths: Sakhalin Island, Russian Far East, Climate Dynamics, 45, 397-405, 2015.

Yadav, R. R., and Bhutiyani, M. R.: Tree-ring-based snowfall record for cold arid western Himalaya, India since AD 1460, Journal of Geophysical Research: Atmospheres, 118, 7516-7522, 2013.

Yadav, R. R.: Tree ring evidence of a 20th century precipitation surge in the monsoon shadow zone of the western Himalaya, India, Journal of Geophysical Research: Atmospheres, 116, 2011.

Yadav, R. R.: Tree ring–based seven-century drought records for the Western Himalaya, India, Journal of Geophysical Research: Atmospheres, 118, 4318-4325, 2013.

634   Yadav, R. R., Gupta, A. K., Kotlia, B. S., Singh, V., Misra, K. G., Yadava, A. K., and Singh, A.

635   K.: Recent wetting and glacier expansion in the northwest Himalaya and Karakoram,

636   Scientific Reports, 7, 6139, 2017.

637   Yao, J., and Chen, Y.: Trend analysis of temperature and precipitation in the Syr Darya Basin in

638   Central Asia, Theoretical and Applied Climatology, 120, 521-531, 2015.

639   Yaqub, M., Eren, B., and Doğan, E.: Flood causes, consequences and protection measures in

640   Pakistan, Disaster Science and Engineering, 1, 8-16, 2015.

641   Yu, J., Shah, S., Zhou, G., Xu, Z., and Liu, Q.: Tree-ring-recorded drought variability in the

642   northern Daxing'anling Mountains of northeastern China, Forests, 9, 674, 2018.

643   Yu, M., Li, Q., Hayes, M. J., Svoboda, M. D., and Heim, R. R.: Are droughts becoming more

644   frequent or severe in China based on the standardized precipitation evapotranspiration

645   index: 1951–2010? International Journal of Climatology, 34, 545-558, 2014.

646   Zafar, M. U., Ahmed, M., Farooq, M. A., Akbar, M., and Hussain, A.: Standardized tree ring

647   chronologies of *Picea smithiana* from two new sites of northern area Pakistan, World

648   Applied Sciences Journal, 11, 1531-1536, 2010.

649   Zang, C., and Biondi, F.: Treeclim: an R package for the numerical calibration of proxy-climate

650   relationships, Ecography, 38, 431-436, 2015.

651   Zhang, Q.-B., Evans, M. N., and Lyu, L.: Moisture dipole over the Tibetan Plateau during the

652   past five and a half centuries, Nature Communications, 6, 8062, 2015.

653   Zhu, L., Li, Z., Zhang, Y., and Wang, X.: A 211-year growing season temperature reconstruction

654   using tree-ring width in Zhangguangcai Mountains, Northeast China: linkages to the Pacific

655   and Atlantic Oceans, International Journal of Climatology, 37, 3145-3153, 2017.

656

657

658

659

660

661

662

663

664

665

666

667

668

669

670

Figure captions

Fig. 1 Map of the weather stations (Drosh station) and sampling sites in the Chitral, HinduKush

Mountains, Pakistan. Different colors represent the elevation changes of the study area.

Fig. 2 Monthly maximum, mean, minimum temperature (^{o}C) and total precipitation (mm) in the

Drosh Weather Station (35.07° N, 71.78° E, 1465 m), Pakistan (1965-2013).

Fig. 3 The regional tree-ring width chronology from 1550 to 2017 in the Chitral, HinduKush

Mountains, Pakistan. The gray area represents the sample depth.

Fig. 4 Pearson correlation coefficients between the tree-ring index of *C. deodara* and monthly

total precipitation (1965-2013) and scPDSI (1960-2013) (a) and monthly maximum and

680   minimum temperature (1965-2013) (b) from June of the previous year to September of the

681   current year. Significant correlations ($p<0.05$) are denoted by asterisks. The "previous" and

682   "current" represents the previous and current year, respectively.

683   **Fig. 5** The scPDSI reconstruction in the Chitral HinduKush Mountain, Pakistan. (a) Comparison

684   between the reconstructed (black line) and actual (red line) scPDSI; (b) The variation of

685   annual (black solid line) and 11-year moving average (red bold line) Mar-Aug scPDSI from

686   1593 to 2016 with mean vale $\pm$ one standard deviation (black dash lines).

687   **Fig. 6** Comparison of our PDSI reconstruction (a) with the precipitation reconstruction (tree-ring

688        $\delta^{18}O$) of Treydte et al. (2006) (b) in northern Pakistan. Purple and brown shaded areas

689   represent the consistent wet and dry periods in the two reconstructions, respectively. Two

690   correlation coefficients ($r = -0.24$ and $r = -0.11$) are the correlation of two original annual

691   resolution reconstruction series and two 11-year moving average series, respectively.

692   **Fig. 7** The Multi-taper method spectrums of the reconstructed scPDSI from 1593 to 2016. Red

693   and green line represents the 95% and 99% confidence level, respectively. The figures

694   above the significant line represents the significant periods of drought at 95% confidence

695   level.

696   **Fig. 8** (a) Spatial correlation between the actual May-August PDSI and the reconstructed May-

697   August scPDSI (1901-2017). (b) The wavelet analysis of the reconstructed scPDSI in the

698   Chitral HinduKush Ranges, Pakistan. The 95% significance level against red noise was

699   shown as a black contour.
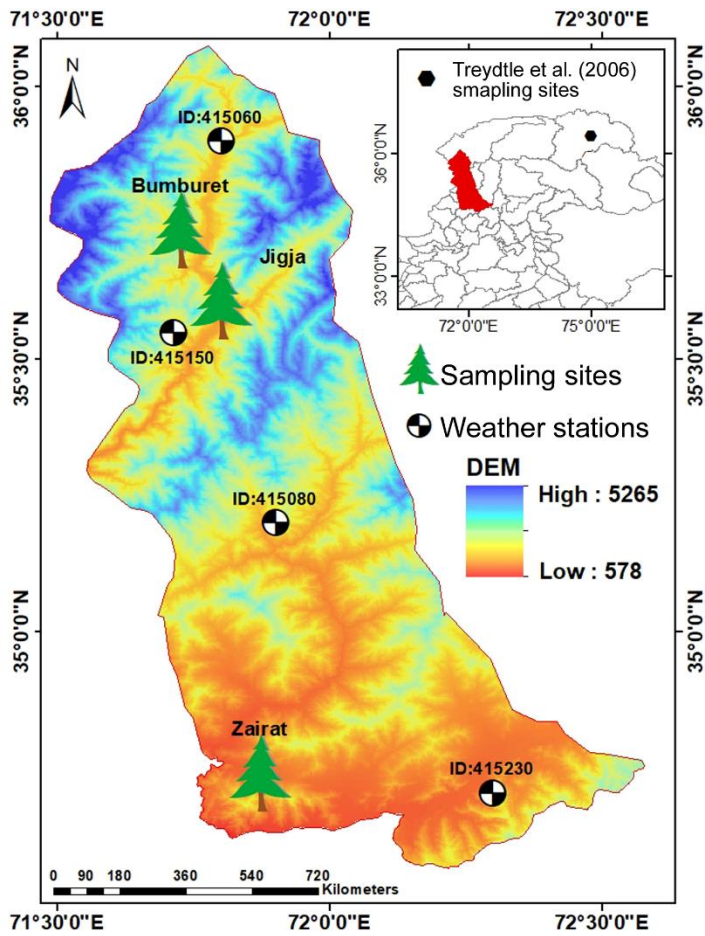
700

701   **Fig. 1** Map of the weather stations (Drosh station) and sampling sites in the Chitral, HinduKush

702   Mountains, Pakistan. Different colors represent the elevation changes of the study area.

703

704
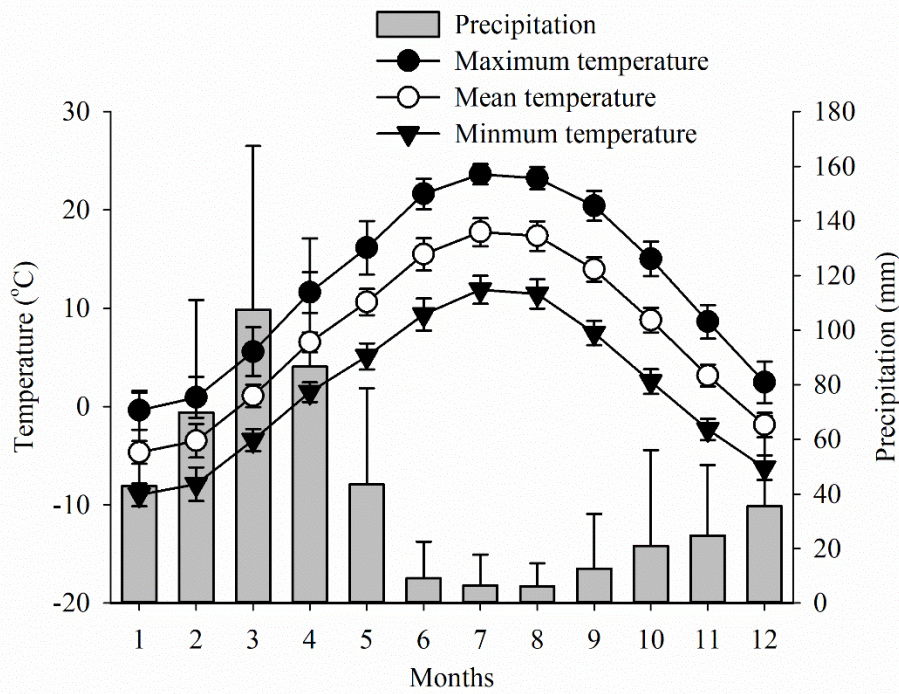
705

706   **Fig. 2** Monthly maximum, mean, minimum temperature (°C) and total precipitation (mm) in the

707   Drosh Weather Station (35.07° N, 71.78° E, 1465.0 m), Pakistan (1965-2013).

708

709
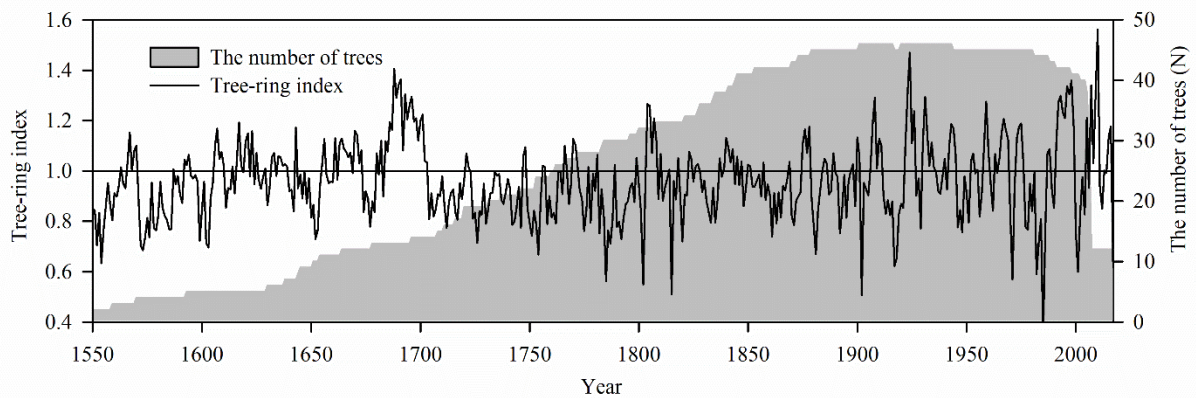
710

711   **Fig. 3** The regional tree-ring width chronology from 1550 to 2017 in the Chitral, HinduKush

712   Mountains, Pakistan. The gray area represents the sample depth.
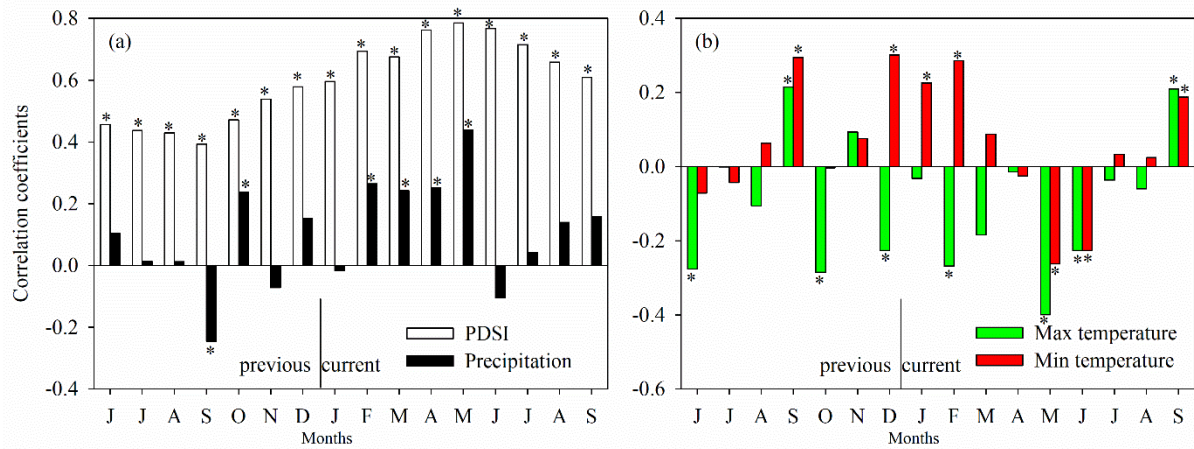
713

Fig. 4 Pearson correlation coefficients between the tree-ring index of *C. deodara* and monthly

total precipitation (1965-2013) and scPDSI (1960-2013) (a) and monthly maximum and

minimum temperature (1965-2013) (b) from June of the previous year to September of the

current year. Significant correlations ($p<0.05$) are denoted by asterisks. The "previous" and

"current" represents the previous and current year, respectively.

719

720

721

722
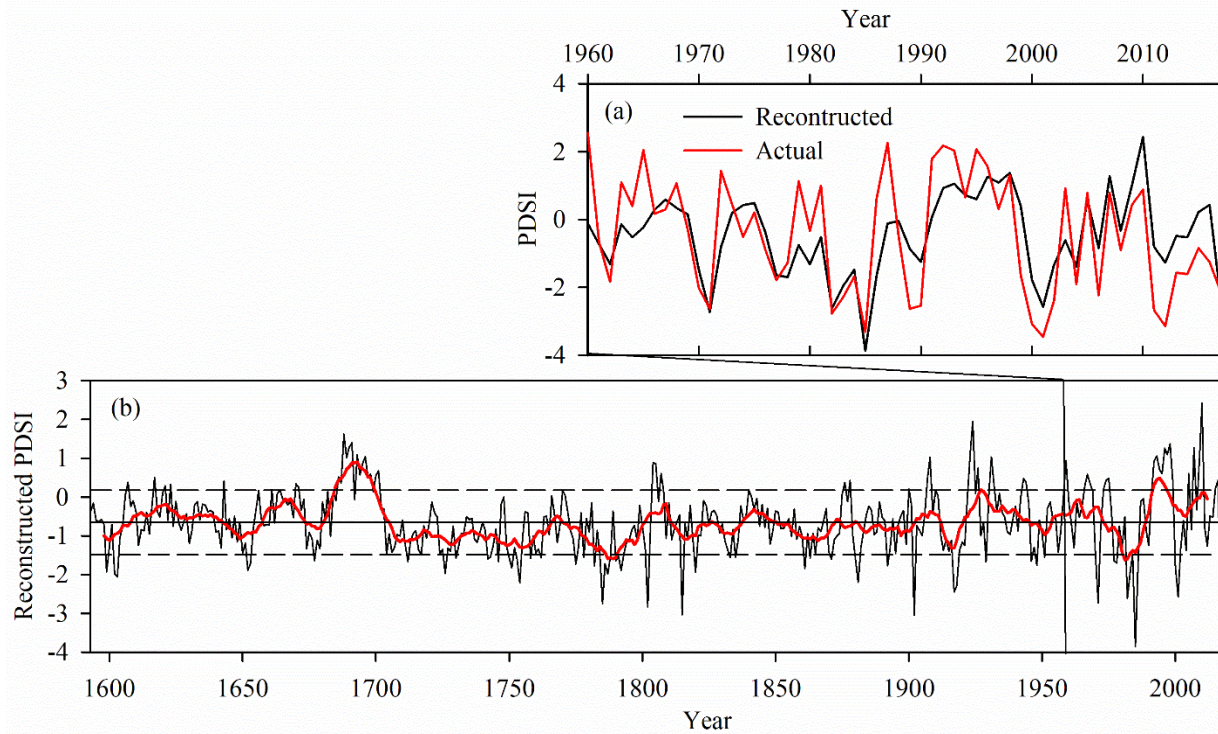
723

Fig. 5 The scPDSI reconstruction in the Chitral HinduKush Mountain, Pakistan. (a) Comparison

between the reconstructed (black line) and actual (red line) scPDSI; (b) The variation of annual

(black solid line) and 11-year moving average (red bold line) Mar-Aug scPDSI from 1593 to

2016 with mean vale $\pm$ one standard deviation (black dash lines).

728
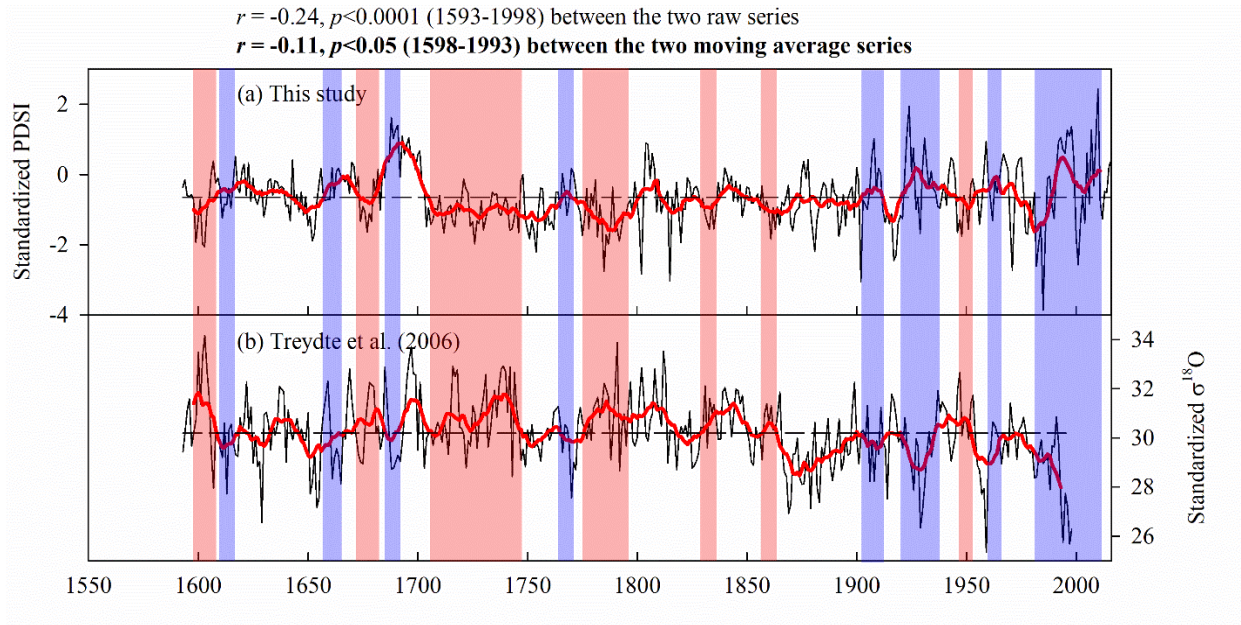
729

Fig. 6 Comparison of our PDSI reconstruction (a) with the precipitation reconstruction (tree-ring

731 $\delta^{18}O$) of Treydte et al. (2006) (b) in northern Pakistan. Purple and brown shaded areas represent

732 the consistent wet and dry periods in the two reconstructions, respectively. Two correlation

733 coefficients (r = -0.24 and r = -0.11) are the correlation of two original annual resolution

734 reconstruction series and two 11-year moving average series, respectively.
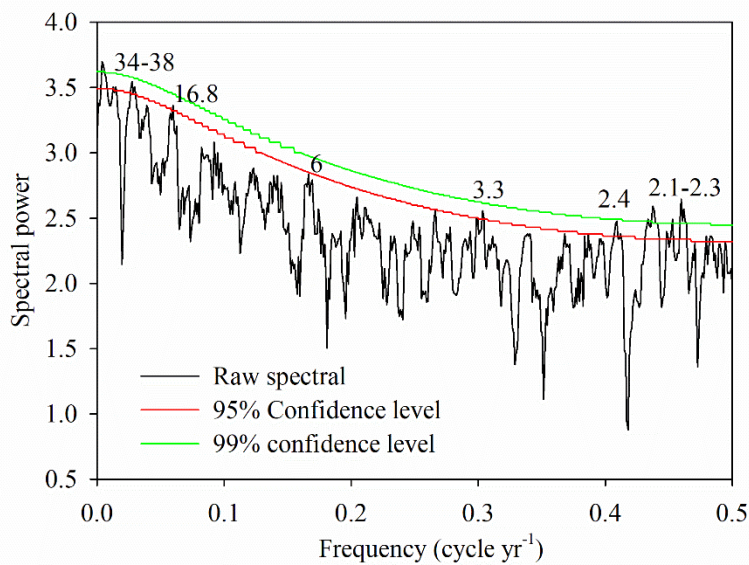
735

736 **Fig. 7** The Multi-taper method spectrums of the reconstructed scPDSI from 1593 to 2016. Red and

737 green line represents the 95% and 99% confidence level, respectively. The figures above the

738 significant line represents the significant periods of drought at 95% confidence level.

739
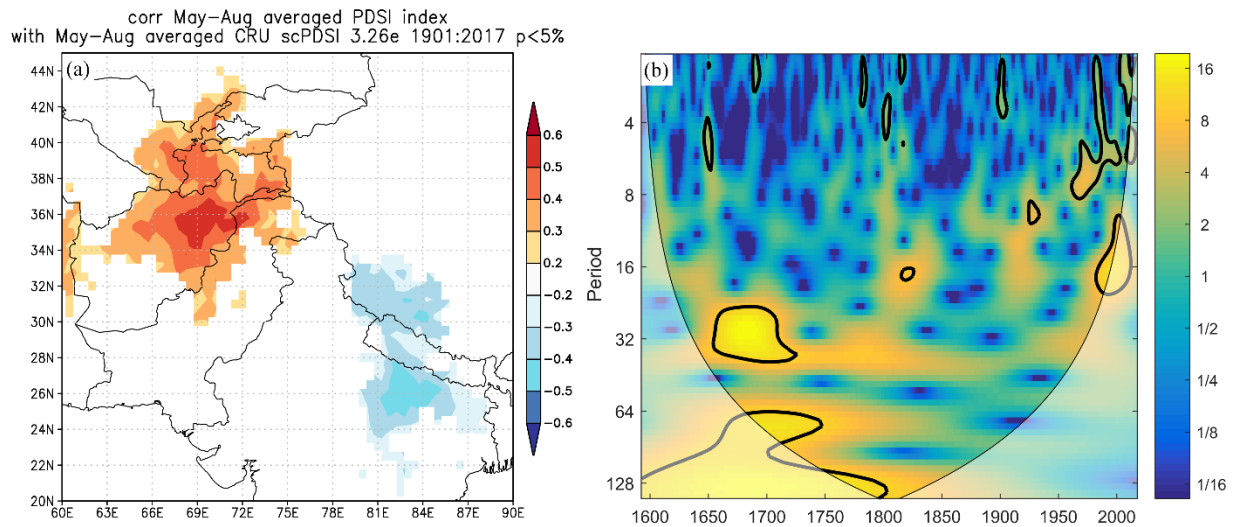
740

741 **Fig. 8** (a) Spatial correlation between the actual May-August PDSI and the reconstructed May-

742 August scPDSI (1901-2017). (b) The wavelet analysis of the reconstructed scPDSI in the Chitral

743 HinduKush Ranges, Pakistan. The 95% significance level against red noise was shown as a black

744 contour.

745

746

747

748
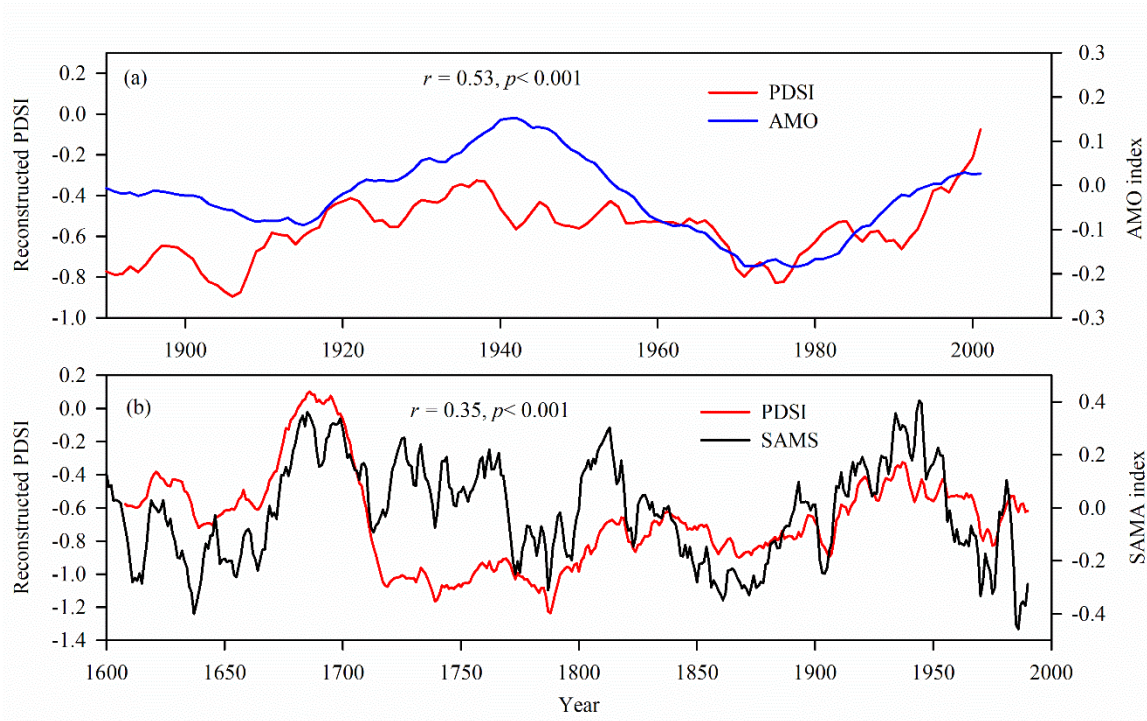
Fig. 9 (a) Comparison of the 31-year moving average series between the reconstructed Mar-Aug scPDSI and the AMO index during the common period (1890-2001); (b) Comparison of the 31-year moving average series between the reconstructed Mar-Aug scPDSI and the JJA-SAMS during the common period (1608-1990).

763 **Table 1.** Statistical test for the tree-ring reconstruction of March-August PDSI in Chitral

764 HinduKush Range of northern Pakistan based on a split calibration-verification procedure.

Calibrations	r	R^2	Verification	RE	CE	ST	DW	RMSE	PMT
1960-2016	0.70	0.49	—	0.44	—	(43, 14)*	1.06*	1.21	10.0*
1989-2016	0.82	0.67	1960-1988	0.61	0.62	(23, 6)*	1.0*	1.72	5.80*
1960-1988	0.73	0.53	1989-2016	0.64	0.62	(24, 4)*	0.98*	1.56	7.42*

765 Notes: RE-Reduction of error, CE-Coefficient of efficiency, ST-Sign test, DW-Durbin-Watson

766 test, RMSE-Root mean square error, PMT-Product means test.

767